AUTOMATIC LASER INTERFEROMETER AND VISION MEASUREMENT SYSTEM FOR STRIPE ROD CALIBRATION

Min Zhao, Qiu-Hong Huang, Ling-Jian Zhu, Zong-Ming Qiu

Xi'an University of Technology, School of Mechanical Instrumental Engineering, Xi'an 710048, China
(✉ zhaomin0710@163.com, +86 139 9114 3528, huangqiuhong@xaut.edu.cn, zlj_zhy@xaut.edu.cn, zongmingq@xaut.edu.cn)

Abstract

In order to calibrate the stripe precision of a leveling rod, an automatic laser interferometer and a vision measurement system were designed by Xi'an University of Technology in China. The rod was driven by a closed-loop control and the data were collected at the stop state to ensure precision. The laser interferometer provided not only the long distance data but also a position feedback signal in the automatic control loop. CCD camera and a vision measurement method were used to inspect the stripe edge position and defect. A pixel-equivalent self-calibration method was designed to improve precision. ROI (*regions of interest*) method and an outline tracing method were designed to quickly extract multiple stripe edges. A combination of the image data with the interferometer data reduces control difficulty and ensures the measurement accuracy. The vision measurement method reached sub-pixel precision and the defective edges were reported. The system can automatically calibrate a stripe leveling rod with a high degree of efficiency and precision.

Keywords: stripe edge, automatic control, laser interferometer, vision measurement.

1. Introduction

A stripe leveling rod with a digital level is employed for automated height surveying [1]. The stripe leveling rod as the carrier of used scale is thereby of special interest. To obtain precise results, the leveling rod must be regularly calibrated [2]. All the stripe positions are detected and compared with a legal meter to determine the rod scale and graduation precision.

A laser interferometer can be used as a superior measurement standard. An optical microscope can be used to collimate the stripe edges. Photoelectric microscope systems were developed in several countries [3–5]. These systems use a slit aperture microscope to detect stripes with the same width as the slit. They are not suited to detect stripes of various widths but only narrow stripes (graduation lines) of equal width.

An automatic calibration system for invar leveling rods has been developed in Taiwan [6–7]. It uses a moving mechanism to move the stripe edges of the leveling rod to the CCD image center, and then records the laser interferometer data. The method is effective compared with manual collimation. For a 3 m length, the uncertainty is 21 μm. Correction of existing collimation deviation by image processing can make collimation easier and improve the measurement precision [8].

Automatic calibration systems based on CCD detection were developed in several countries [9–10]. The image and the interferometer data are obtained while the rod is moving. It takes about 90 minutes to calibrate a rod [10]. Automatic calibration systems which can calibrate leveling rods and find defective edges with high efficiency and high precision are highly desired in China. However, so far no automatic calibration system exists in China.

An automatic calibration system for stripe leveling rods is presented in this paper. The rod moves and stops automatically and rapidly. The image and the interferometer data are collected at the stop state to ensure precision. Several stripe edges are inspected by the vision measurement simultaneously. The system is highly efficient and precise. The system can simultaneously calibrate the leveling rod and report defective edges. This paper presents the automatic calibration principle and the vision measurement method.

2. Automatic calibration principle

2.1. System introduction

The calibration system was designed in Photoelectric Measurement Technique Lab at Xi'an University of Technology in China. The basic setup of the calibration system is schematically shown in Fig. 1. It mainly consists of a rod carrier section (including a base, a guide rail, a screw and a worktable), a motion control section (including a motor, a drive controller and a drive card), a vision measurement section (including a light source, an illumination controller, a microscope and a CCD camera), a laser interferometer (including a reflector, a beam splitter, a laser head, an interferometer controller and an interferometer board), and a computer.
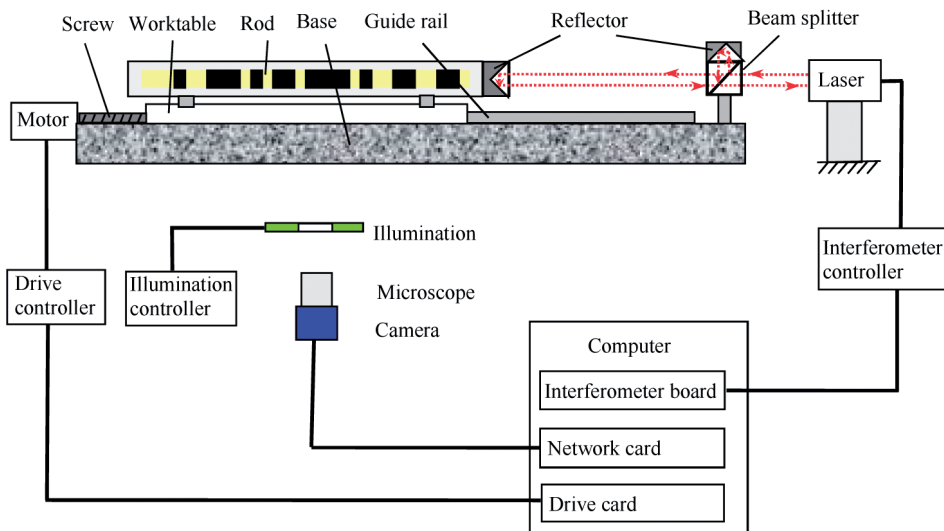

Fig. 1. A schematic of the automatic calibration system.

The rolling screw and the linear sliding guide rail are installed on a marble base. The motor drives the screw directly, driving the worktable and the rod mounted on it to move along the guide rail. The computer controls the motion of the rod via the motion control section. The positioning control is realized by a closed-loop control. The laser interferometer is the positioning sensor in the closed-loop control system.

The laser interferometer is employed to calibrate the leveling rod. According to the Abbe principle, the optical axis of the reflector coincides with the direction of the rod movement. The reflector is fixed at the starting end of the calibrated rod, so that the moving distance of the rod can be obtained precisely [11−12]. The laser interferometer responds quickly; it can meet the requirement of real-time measurement and rapid positioning control. The interferometer data can be obtained by the computer via its interferometer board.

The vision measurement section detects the stripe edges which moved into its field of view. Due to the manufacturing process, the stripe elements are a few micrometer thick [13]. Two LED light sources illuminate the path along the stripe direction, thus avoiding the shadowing effect of the stripe elements and highlighting the edge. The green light was chosen to obtain the best response characteristics of CCD [14]. The microscope was designed with a large diameter and a long focus. The large diameter corresponds with higher optical resolution, whereas the long focus corresponds with minimal optical distortion. An object tele-centric beam path has been adopted, which effectively improves the measurement accuracy [15]. The CCD camera takes the stripe images and transfers them to the computer by its network card. The stripe edges are detected and the collimation deviations are obtained by image processing.

The rod is installed in the rod carrier section. The motion control section controls the motion of the rod. The laser interferometer measures the moving distance. The vision measurement section obtains the collimation deviation of the detected stripe edge. The stripe edge position is a combination of the moving distance and the collimation deviation. The calibration system is controlled by an industrial computer with Windows XP as the operating system.

2.2. Automatic calibration method

The calibration process is shown in Fig. 2. The motor moves the rod. The moving distance of the rod is obtained by the laser interferometer in real time. The rod continuously moves in equal distances and then stops. When the rod stops, the laser interferometer measures the moving distance. At the same time, a section of the stripe image is taken with the CCD camera and saved in the computer memory. Then, on consecutive moves and stops of the rod, a series of stripe images are being saved in the computer, along with their corresponding interferometer data. This process continues until all of the images and the data of the rod are collected. The calibration process is accomplished automatically by the calibration system, without a need of the operator's assistance, once the process started.

The series of images are automatically processed in succession to obtain the stripe edge position in the image. The edge position is correlated with the reference position (set to the image center) to obtain the collimation deviation. By adding the moving distance of the rod measured by laser interferometer, the edge position from the start position can be determined.

$$X = L + (D - D_0) \times k, \qquad (1)$$

where: X is the measured edge position in mm, L is the interferometer value in mm, D is the edge position in the image in pixel, D_0 is the reference position in pixel, k is the actual size projected onto each pixel in mm/pixel (pixel equivalent). k can be obtained by pixel calibration.

The rod moves and stops automatically and rapidly. Since the images and the interferometer data are collected in the stop state, the motion blur is avoided and the correspondence between the collected images and interferometer data is guaranteed.

Combining the image data (the stripe edge position in the image) with the interferometer data, only a detected edge needs to exist in the field of view. The method does not require precise optical collimation for the detected edge, so the measurement is rapid. The method is not limited by the code width, so it can be used to measure leveling rods of various coding.

Measuring with the constant spacing requires only the spacing to be smaller than the field of view to ensure a certain control redundancy. The method does not require accurate positioning of the rod, so the control is easy to implement.

Collecting the images followed by calculating the data saves the original image and data, which can be used for documentation of the rod.
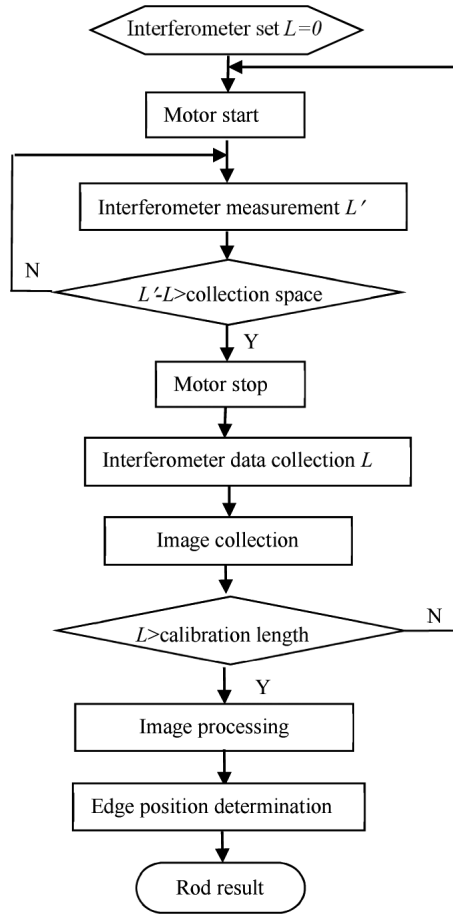
Fig. 2. The automatic calibration process.

2.3. Pixel-equivalent self-calibration

To calculate the edge position according to (1), the pixel needs to be calibrated to determine the pixel equivalent [16]. Pixel calibration is usually performed before the measurement. Due to small fluctuations of the invar surface where the stripe is carved, the pixel equivalent is somewhat different in different sections. Therefore, the pixel equivalent of one section is not the best representation of the pixel equivalent of the whole rod. Pixel calibration along the whole rod improves the accuracy, but is very time-consuming.

Because the field of view is larger than the collection spacing, some of edges are collected by two adjacent images simultaneously. An edge that is collected by two images can be used to determine the pixel equivalent. The detected edge position in one image is D_1 and in the adjacent image is D_2, while the interferometer values are L_1 and L_2, respectively. The detected edge position X does not change with the collection position.

$$X = L_1 + (D_1 - D_0) \times k = L_2 + (D_2 - D_0) \times k. \tag{2}$$

Then,

$$k = (L_2 - L_1) / (D_1 - D_2). \tag{3}$$

This pixel calibration method requires only the collection space to be smaller than the field of view, and each stripe edge to be collected twice. Many edges that are collected twice can be used to determine the pixel equivalent by using the average of the calibration results. The average over the whole rod can greatly improve the accuracy. This method can accomplish self-calibration in the measurement process, making the measurement process more simple and convenient.

After pixel equivalent calibration, every stripe edge position on the rod can be obtained by (1).

3. Vision measurement

In the CCD camera, the pixel count is 1280 × 960 and the pixel size is 4.65 μm × 4.65 μm. The microscope magnification is approximately 1x. The size of the view field is approximately 6 mm × 4.5 mm. There may be several edges in an image, as shown in Fig. 3a. To obtain every edge precisely, a special image processing method was designed. The process is as follows: ROI (*regions of interest*) extraction, local segmentation, outline following, plausibility check and edge localization.

3.1. ROI extraction

The general method of extracting the edges is dealing with the global image. The global method will not work well when faced with different edge properties or uneven illumination. The idea is to extract *regions of interest* (ROI) and make calculations only in those ROIs [17]. The precision and efficiency will be improved at the same time.

As there may be several edges in an image, all the regions and properties (bright – dark or dark – bright transition) of every edge should be first determined. The ROIs are close to the edges along the column direction, so the column property is used to locate the regions. The average grey value of every column position x is $I(x)$.

A double threshold method was designed. The high threshold T_h was set at 80% (the low one T_l – at 20%) of pixels in the magnitude histogram. Experimental results have shown that if the high threshold is lowered and the low threshold increased, the filter will be more sensitive to the grey-level variations. However, it will be also more sensitive to noise.

If T_h and T_l are close enough, this means no edge exists in the image and no further processing is needed.

If $I(x-\varepsilon) > T_h$ and $I(x+\varepsilon) < T_l$, this means an edge located near x with bright – dark transition (left edge).

If $I(x-\varepsilon) < T_l$ and $I(x+\varepsilon) > T_h$, this means an edge located near x with dark – bright transition (right edge).

The parameter e is related to the tilt of the CCD, which is intentional and can be determined. Then the ROIs are determined around x (near the edge position) with suitable widths.

3.2. Local segmentation

After determination of the ROIs , image segmentation in these small regions can improve both accuracy and efficiency. We look at every region as a whole and use the global threshold in every ROI [22].

Let us consider that we have an image region with grey levels gand its normalized histogram (*i.e.*, for each grey-level value i, $p(i)$ is the normalized frequency).

Assuming that we have set the threshold at *T*, the normalized fractions of pixels that will be classified as the background and object ones, will be:

$$
\begin{cases}
q_b(T) = \sum_{i=1}^{T} p(i) \\
q_o(T) = \sum_{i=T+1}^{g} p(i)
\end{cases},
\tag{4}
$$

where: $q_b(T) + q_o(T) = 1$. The between-class variance is:

$$
\sigma_B^2 = \frac{[u(T) - uq_b(T)]^2}{q_b(T)q_o(T)},
\tag{5}
$$

value, once the threshold is set to *T*.

Let us start from the beginning of the histogram and test each grey-level value for the possibility of being the threshold T that maximizes σ_B^2 .

The result of local segmentation of Fig. 3a is shown in Fig. 3b. Every ROI is segmented using its own threshold, whereas other regions are untouched. After local segmentation, every edge is obvious.

Fig.3. ROI extraction and local segmentation: a) several edges in an image; b) local segmentation in ROI; c) the detected stripe edges.

3.3. Outline tracing

Some of the edges have noise and faults, as shown in Fig. 5a. An outline tracing algorithm was designed to search the edge directly, avoiding the difficulty of noise removal. The outline tracing process is as follows.

Every binary ROI is scanned from the top to bottom, beginning from the left and right, respectively. The outline tracing of the left edge is shown in Fig. 4. From the left (white area) the scan stops when the first black pixel appears. The pixel position is recorded as *m*. From the right (black area) the scan stops when the first white pixel appears. The pixel position is recorded as *n*. If *m* ≠ *n*, the scan moves to the next row; if *m* = *n*, the pixel point must be the outline point, so the scan stops.

Such a point A must exist in the ROI, as shown in Fig. 4. After that, the outline is searched up from A and down from A, respectively. According to the outline continuity, the outline point of every row is traceable. When tracing down the outline, consecutive points are searched for, according to the priority: the left neighbor, the left neighbor below, the neighbor below, the right neighbor below, the right neighbor. However, a consecutive point does not indicate an outline point. For the left edge, if the left neighborhood of the consecutive point is disconnected, this point is the outline point. Otherwise, the search continues until the left neighbor of the point is

disconnected. In Fig. 4, tracing down from point A gets A→B1→C1 and tracing up from point A gets A→D1→E1. Thus, the consecutive outline points are E1→D1→A→B1→C1.
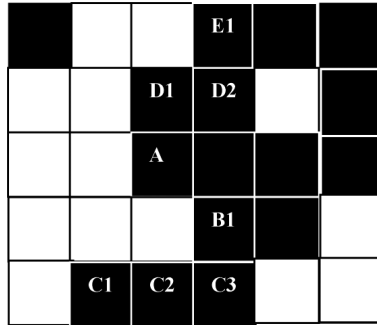

Fig. 4. The outline tracing graph.

The outline tracing result of Fig. 3b is shown in Fig. 3. The white outlines are the detected stripe edges.

After ROI extraction, local segmentation and outline tracing, the result of Fig. 5a is shown in Fig. 5b. For the left edge, the dirt is eliminated by outline tracing. For the right edge, the edge fault is obvious and requires further processing.

3.4. Plausibility check

The detected edges pass then through the plausibility check, to find dirt, scratches and defects. The method is as follows.

A line represented by the equation $x = b \times y + b_0$ is fitted to the stripe edge points using the least-squares regression, which minimizes the sum of the squares of perpendicular distances between the edge points and the line model. b and b_0 are given by:

$$
\begin{cases}
b = \dfrac{n \sum\limits_{i=1}^{n} x_i y_i - \sum\limits_{i=1}^{n} x_i \sum\limits_{i=1}^{n} y_i}{n \sum\limits_{i=1}^{n} y_i^2 - (\sum\limits_{i=1}^{n} y_i)^2} \;, \\
b_0 = \dfrac{1}{n}(\sum\limits_{i=1}^{n} x_i - m \sum\limits_{i=1}^{n} y_i)
\end{cases}
\tag{6}
$$

where: x_i, y_i stand for the pixel position of the edge in the image, n is the quantity of the pixel point.

The residual error and the standard deviation can be expressed as:

$$
\begin{cases}
v_i = x_i - (by_i + b_0) \\
\sigma = \sqrt{\sum\limits_{i=1}^{n} v_i^2 / (n-2)}
\end{cases}.
\tag{7}
$$

If $v_i > 3\sigma$, this means that an outlier exists and should be excluded from the edge data.

The least-squares regression line is not the optimal result if there are some outliers present in the edge data. So, we continue using the least-squares regression and outlier judgment until

no outliers exist on the edge. If an edge has many outliers, the edge is a defective one and its position on the rod is reported.

The processing result of Fig. 5b is shown in Fig. 5c. It is observed that the edge was acquired without dirt and defects. And the defective edge should be reported.
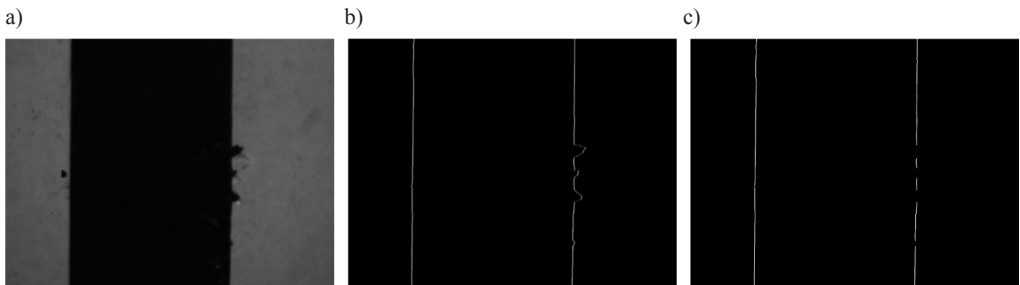
a)   b)   c)

Fig. 5. Outline tracing and the plausibility check: a) edges with noise and fault; b) after outline tracing; c) after the plausibility check.

3.5. Edge localization

To improve the result, the CCD chip was intentionally tilted against the vertical direction of the rod movement by a well-calibrated amount to allow sub-pixel edge detection. If an irregular edge is regarded as a regular edge with a space disturbance, probability and statistics subdivision can be applied to improve the image resolution [18]. The implemented algorithms enable localization of contours with the accuracy of 1/10 of a pixel, *i.e.*, less than 0.5 μm.

4. Experiment and results

An overview of the calibration system is shown in Fig. 6. The measurement system was tested by the experts from China's national metering bureau.
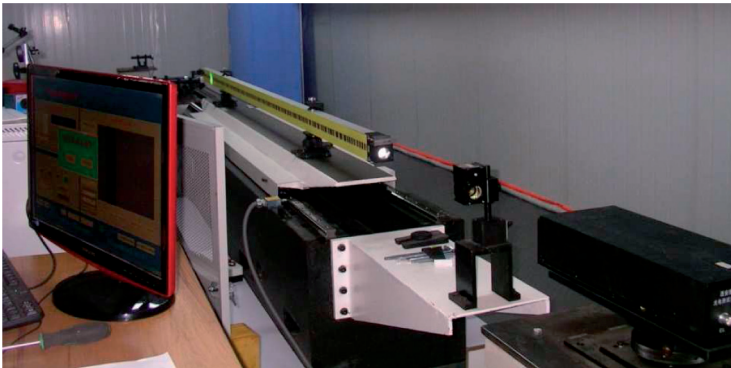

Fig. 6. An overview of the measurement system.

4.1. Vision measurement experiment

The computer controlled the leveling rod, moving it in small distances. The same edge was measured several times at different image positions. At the first position, the interferometer was set to zero. At every subsequent position, the image and the interferometer data were collected.

The edge position in the image was obtained by the ROI method presented in Section 3. Comparing the image data with the interferometer data, the vision measurement precision can be determined. The measurement data is shown in Fig. 7a. There is a good linearity between the image data and the interferometer data.

The real edge position was obtained by combining the image data with the interferometer data using (1). The result is shown in Fig. 7b. There is a good consistency for the same edge measured in different positions. The standard deviation is 0.42 μm.

The experiment proves that a combination of the image data with the interferometer data ensures the measurement accuracy. The experiment results also prove that the combination method is reliable, if only the detected edge exists in the field of view, so the control is easy to implement.

The experiment indicates that the image processing method reaches the sub-pixel precision. If the global method is used to obtain the edge position in the image, the standard deviation is 0.9 μm. The precision is greatly improved with use of the ROI method.

700 images of a 3 m rod were chosen to test the image processing speed. The global method took 270 seconds, while the ROI method took only 70 seconds under the same conditions. The efficiency is greatly improved with use of the ROI method.
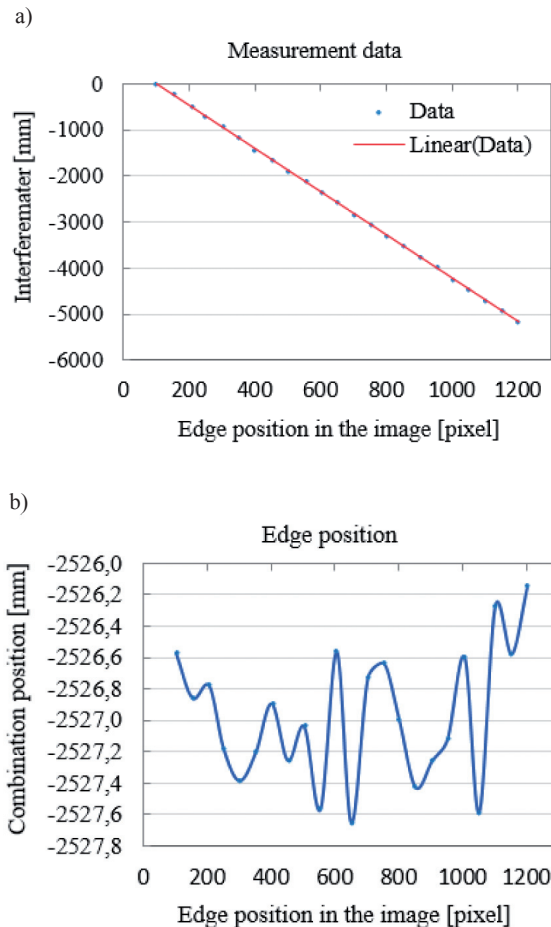
a)

b)

Fig. 7. Measuring an edge at different positions: a) comparing the image data
with the interferometer data; b) the data combination.

4.2. Calibration of the Leveling Rod

The rod scale and the graduation precision of a leveling rod were measured according to JJG8-1991 (national level rod metrological detection procedures) [19].

After installing the leveling rod and adjusting the equipment, calibration of the leveling rod began. The measurement process was accomplished automatically by the calibration system, needing no operator's assistance. It took 28 minutes to measure back and forth for a 3 m rod. After the measurement, the result was obtained automatically, as shown in Table 1. Part of the stripe position error is shown in Fig. 8.

Table 1. The measurement result of a rod.

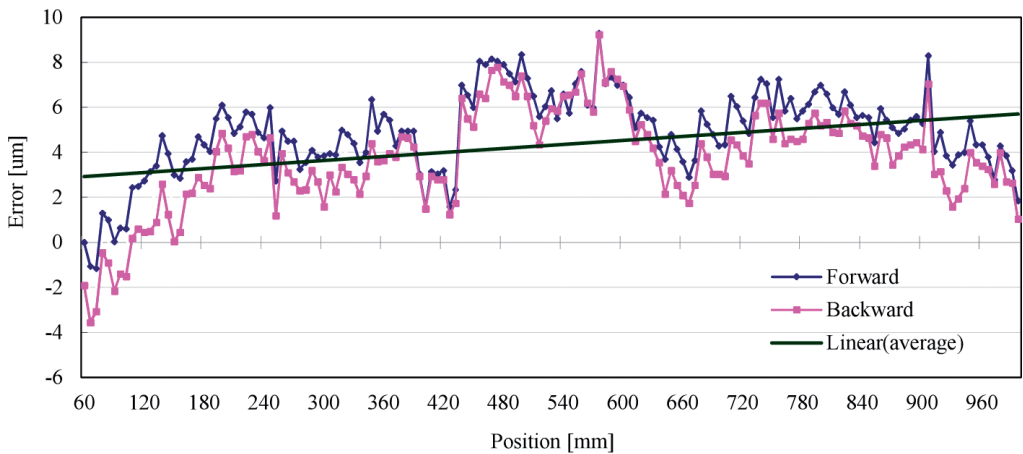| Item	Result
misclosure of round	1.9 μm
vision measurement precision	0.5 μm
rod graduation precision	2.0 μm
rod scale	1000.0031 mm

Fig. 8. Part of the stripe position error.

The misclosure of the round is 1.9 μm, which shows a good stability of the measurement system. The standard deviation of stripe width between the forward and backward measurements is 0.5 μm, which shows a good consistency of the measurement system. Because of the stability and consistency of the measurement system, the rod result (graduation precision and rod scale) is reliable.

The detected rod is a high precision Topcon rod made in Japan. The measurement result of the rod is consistent with the given value. This indicates that the detection system is very precise and can meet the measurement requirements for high precision rods.

Some rods made by Chinese manufacturers were tested. The defective edges were found in a timely manner before these rods went into market. These rods require further testing after repairing their defective edges. The system provides quality assurance for the manufacturers.

5. Conclusions

An automatic calibration system for stripe leveling rods was designed and presented in this paper. The system configuration, the automatic calibration principle, and the vision measurement method were described in detail. The stripe rod was driven by a closed-loop control and the data were collected in the stop state. A laser interferometer was used not only to determine the length, but also as a positioning sensor. The stripe edge position was obtained by combining the image data with the interferometer data. The data combination method reduces control difficulty and ensures the measurement accuracy.

The measurement system was tested by the experts from China's national metering bureau.

The standard deviation of vision measurement is less than 0.5 μm. The overall precision of the system is better than 3 μm. The system can measure the highest precision stripe rods. It takes only 28 minutes to measure a 3 m rod, so it can be used for batch calibration. It can detect defective edges, providing quality assurance for manufacturers. The system currently works well in several survey agencies and rod manufacturers in China.

Acknowledgements

References

[1] Liu, J.N., Ye, X.M., Yang, S.J. (2009). The overview of digital electronic level principle. *Journal of Electronic Measurement and Instrument*, 23(7), 89–94.

[2] Gassner, G.L., Ruland, R.E. (2006). The SLAC Comparator for the Calibration of Digital Leveling Equipment. *9th International Workshop on Accelerator Alignmen*t.

[3] Penzes, W.B., Allen, R.A., Cresswell, M.W., Linholm, L.W. (2000). Teague EC. A new method to measure the distance between graduation lines on graduated scales. *IEEE Transactions on Instrumentation and Measurement*, 49(6), 1285–1288.

[4] Takalo, M. (2000). On automation in precise height determination. *Acta Polytechnica Scandinavica*, 119, 7–24.

[5] Li, X., Zhao, N.N., Guo, J.J. (1990). On automatic measurement system of invar grade rod. *Acta Geodetic Cartographic Sinica*, 19(2), 130–137.

[6] Chen, C.S., Wu, C.T., Chang, M.W., Chang, W.C. (2008). Establishing an invar leveling calibration system. *Journal of the Chinese Institute of Engineers*, 31(5), 861–866.

[7] Wu, C.T., Chen, C.S., Chang, M.W. (2013). Uncertainties in the Calibration System for Invar Leveling Rods. *Journal of Applied Science and Engineering*, 16(1), 69–78.

[8] Zhao, M., Qiu, Z.M., Huang, Q.H., Zhu, L.J. (2008). Code-bar grade rod measurement by vision collimation and laser interferometry. *Optics and Precision Engineering*, 16(3), 537–542.

[9] Peter, W., Karl, F. (2006). A New CCD-based Technique for the Calibration of Leveling Rods. *XXIII FIG Congress, Munich*, Germany.

[10] Woschitz, H., Gassner, G., Ruland, R. (2007). SLAC vertical comparator for the calibration of digital levels. *Journal of Surveying Engineering*, 133(3), 144–150.

[11] Kim, J.A., Kim, J.W., Kang, C.S. (2010). An interferometric Abbe-type comparator for the calibration of internal and external diameter standards. *Measurement Science and Technology*, 21(7).

[12] Birch, K.P., Downs, M.J. (1993). An Updated Edlén Equation for the Refractive Index of Air. *Metrologia*, 30, 155–162.

[13] Takao, O., Tetsuo, S. (2010). Manufacturing processes and products of bar and wire rod in JFE steel group. *JFE Technical Report*, 15, 1–3.

[14] Djite, I., Magnan, P., Estribeau, M. (2010). Modeling and measurements of MTF and quantum efficiency in CCD and CMOS image sensors. *Proc. of SPIE*, 7536.

[15] Bloch, S., Betensky, E. (2001). Telecentric zoom lens used in metrology applications. *Proc. of SPIE*, 4487, 42–52.

[16] Huang, Q.H., Zhao, M., Qiu, Z.M. (2007). Online self-calibration method of code-bar grade rod imaging system. *Journal of Optoelectronics Laser*, 18(3), 353–355.

[17] Wu, T., Qin, K. (2012). Data field-based transition region extraction and thresholding. *Optics and Lasers in Engineering*, 50,131–139.

[18] Zhao, M., Qiu, Z.M., Huang, Q.H. (2002). A Method for Improving Resolution Power of Image Measurement. *Journal of Xi'an University of technology*, 18(1), 80–83.

[19] JJG 8-1991: Verification regulation of level rod. National metrological verification regulations of People's Republic of China.